Supplemental Data

Energetic coupling between an oxidizable cysteine and the phosphorylatable N-terminus of Human Liver Pyruvate Kinase

Todd Holyoak, Bing Zhang, Junpeng Deng, Qingling Tang, Charulata B. Prasannan and Aron W. Fenton

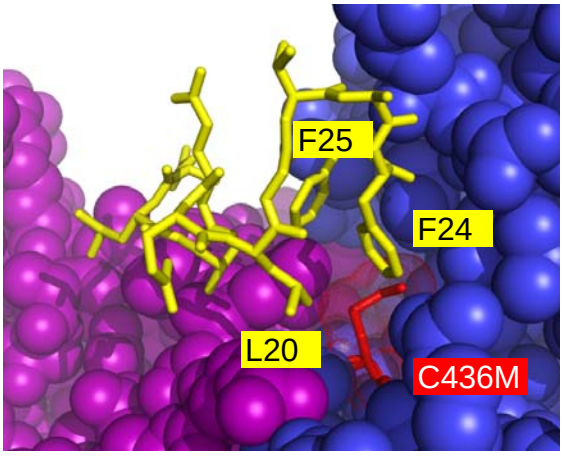

Figure S1. A) Cysteine 436 is conserved in mammalian L/R-PYK isozymes as well as the two M-gene products. Cys436 is highlighted. B) The oxidation steps of sulfenic acid. The addition of a single hydroxide is reversible, whereas additional oxidations are not reversible. C) C338A and C370A continue to show sensitivity to the concentrations of H_2O_2 used in Figure 3.

A

Rat L	VEASFKCCAAA
Mouse L	VEASFKCCAAA
Human L	VEAAFKCCAAA
Bovine L	VEAAFKCCAGA
Rat M_2	VEASFKCCSGA
Rat M_1	VEASYKCLAAA
Rat R	VEASFKCCAAA

B

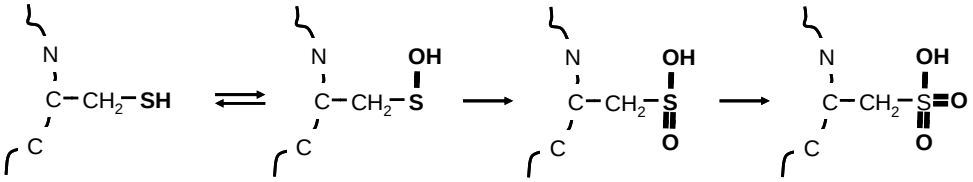

C

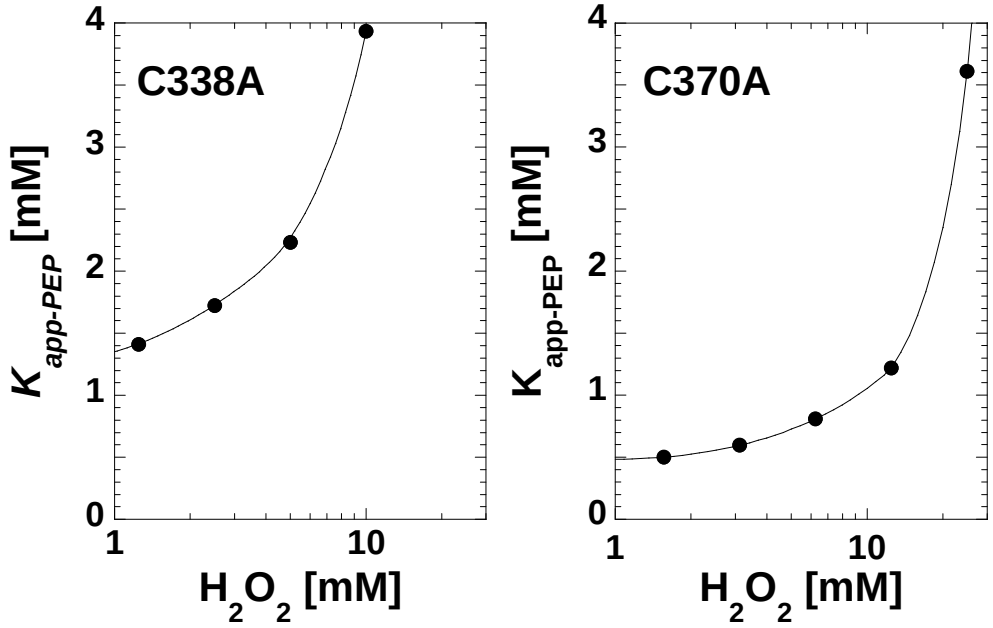

Figure S2. A helical wheel for residues 11-24, consistent with the periodic nature of data in Figure 5. Created by "Helical Wheel Projections" created by Don Armstrong and Raphael Zidovetzki, modified by Jim Hu.

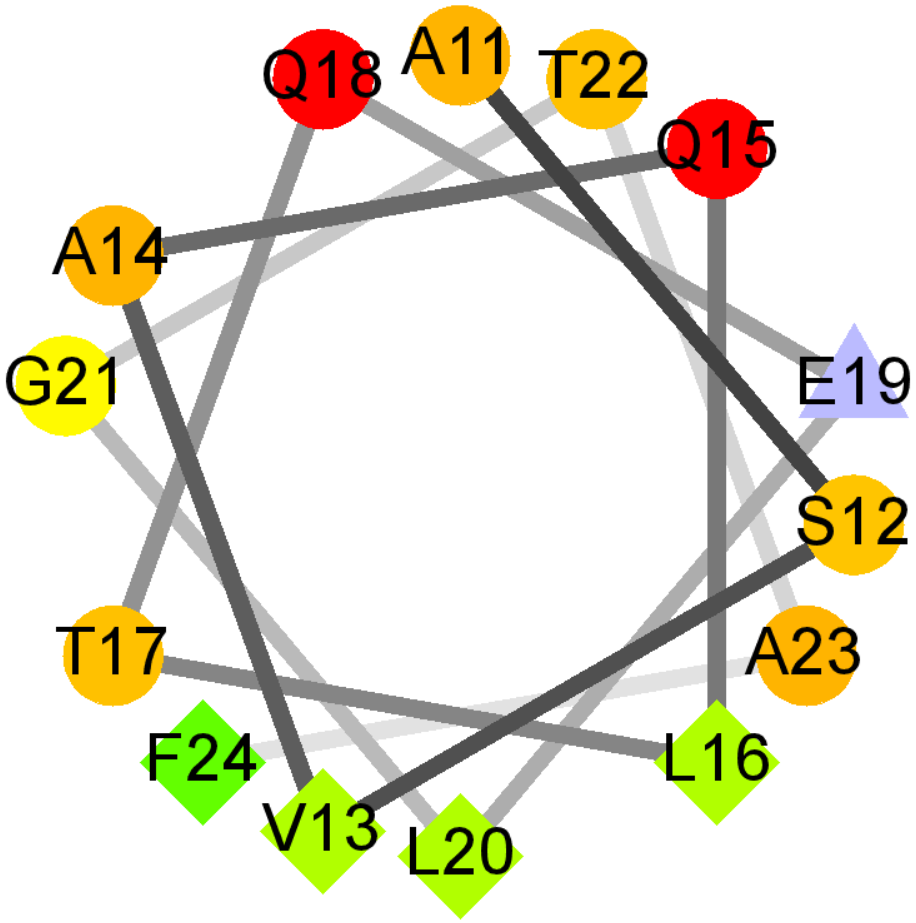

Other notable observations: the elusive ATP allosteric binding site

Our original structural study was initiated with a second goal, to identify the location of a potential ATP allosteric binding site. ATP is typically listed as an allosteric regulator of L-PYK. Consistent with this potential role, addition of ATP reduces the apparent affinity of L-PYK for PEP, with no change in V_{max} activity (*1*). However, experimental designs to study ATP inhibition of this enzyme are challenging. L-PYK requires two divalent cations for activity: one bound in the protein's active site and one bound to the active site nucleotide. PEP coordinates to the protein bound divalent cation. It is currently unknown if the regulatory nucleotide binds in free ATP form or as the Mg-ATP complex. Additions of ATP can chelate divalent metal such that there are insufficient quantities of metal to fulfill the active site divalent requirements. Such chelation could result in inhibition, although the effects on turnover rate and/or substrate binding affinities are unclear due to the multifaceted role of divalent cations. In addition, ATP is expected to bind competitively with ADP and PEP when present at sufficiently high concentrations. As a result, varying ATP alone, as a means of characterizing potential allosteric regulation, is not an effective experimental design. In fact, Irving and Williams previously challenged that ATP is not an allosteric effector of L-PYK when the concentration of free Mg^{2+} is maintained (*2*). As an alternative to varying ATP alone, we previously varied ATP as a mixed solution containing equal molar concentration of ADP, to prevent competitive inhibition. This mixture also contained $MgCl_2$ concentration equal to the combined ATP/ADP concentration, an effort to prevent effects that result from loss of Mg^{2+} binding in the active site. These efforts allowed monitoring of an inhibition that is pH dependent and consistent with previously reported allosteric inhibition by ATP (*3*). However, we have recently demonstrated that changes in anion type and concentration also modifies PEP affinity (*4*); changes in Cl^- concentrations are inherent

to the experimental design we previously used (*3*). This may further challenge the ability to devise a properly controlled experiment to evaluate if inhibition upon ATP addition is a result of allostery.

Little insight into a potential allosteric role for ATP is gained by a review of structural studies of the various PYK isozymes. The only structure that claims potential identification of a regulatory nucleotide binding site is of muscle PYK (M_1-PYK). However, this speculative identification is based solely on a low resolution difference map that results upon the addition of ADP, not ATP (*5*). Furthermore, studies that have evaluated the ability of ATP to regulate M_1-PYK indicate, at best, marginal responses that range from slight activation to slight inhibition (*6-11*). Our efforts fail to detect ATP inhibition in M_1-PYK (Supportive Information). As a further argument against ATP regulation in M_1-PYK, higher resolution structures with nucleotide bound in the active site do not contain electron densities for nucleotide outside of the active site (*12*). Nucleotides are also absent outside of the active site in structures of human M_2-PYK (reference 3GR4 in the protein data bank) or *Leishmania mexicana* PYK (*13*), even though nucleotides were included in the respective crystallization mixtures.

Despite efforts to ensure that monitored regulatory properties are correctly ascribed to allosteric inhibition by ATP, the inherent difficulty in experimental design, the small regulation relative to that caused by other effectors (*3*), and the lack of an identified binding site on the protein combine to undermine confidence that ATP is a true allosteric regulator of L-PYK. Therefore, one of the reasons for initiating the current crystallographic studies was an attempt to co-crystallize the regulator ATP bound to human L-PYK.

The only electron density for which ATP might contribute is located between two tetramers (Supportive Information). The density is best satisfied by modeling the adenine ring at

50% occupancy in two overlapping orientations, leaving the ribose ring and phosphate moieties disordered. The position of this density at the interface between two tetramers might imply that inhibition by ATP results in altered oligomeric state; octomeric states have not been reported for this isozyme. Even more inconsistent with a regulatory role is the fact that the γ-phosphate was not ordered (i.e. bound to the protein) to offer selection between ADP and ATP.

Residues surrounding the electron density just described include R68, E89, N104, and E94. Six mutations were introduced at these 4 positions to probe for allosteric ATP function. The magnitude of the allosteric coupling caused by the ATP/ADP/Mg^{2+} addition was evaluated using a linked-function analysis (*3, 14, 15*). Moderate perturbations (R68K and E89D) and complete side chain removal (R68A, E89A, N104A, and E94) modified PEP affinity, but have minimal influence on the response of PEP affinity to varying ATP/ADP/Mg^{2+} (Supportive Information). Based on the later observation, we conclude that binding of the adenine ring at the interface of two tetramers is a crystallization artifact and is not relevant to regulation by ATP. The presence of neucleotide concentrations that are sufficient to cause artifact binding without binding to an allosteric site are consistent with (but not conclusive of) the idea that ATP does not act as an allosteric inhibitor.

Figure S3. Lack of ATP inhibition of rabbit M_1-PYK vs. inhibition of human L-PYK

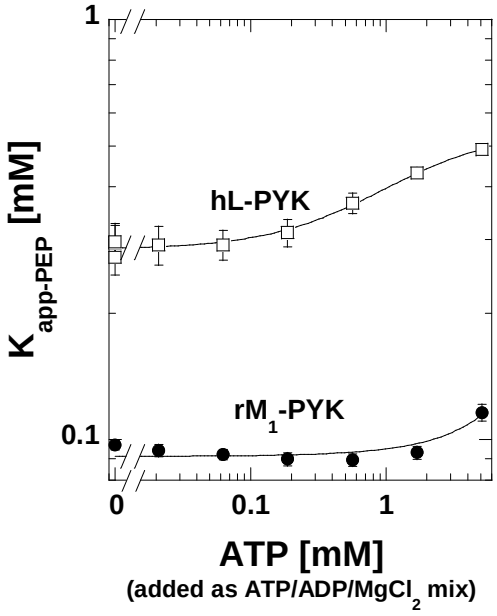

Figure S4. A) The relative location of a putative ATP binding site. The tetramer present in the ASU and its symmetry mate are rendered as ribbons. The individual subunits, A, B, C and D are colored pink, blue, cyan and corral, respectively. The bound ATP, modeled in two conformations is located at the A-D interface. An arrow is pointing towards the ATP molecule, which is rendered as sticks and colored by atom type. B) The response of $K_{app\text{-}PEP}$ to ATP. ATP was added as a ATP:ADP:$MgCl_2$ (1:1:2 molar ratio) as previously described (*3*). No effort has been made to distinguish the response of wild type, R68K, R68A, E89A, N104A, E94A, or E89D since each of these proteins continues to display a response to ATP. Lines represent the best fits to Equation 1.

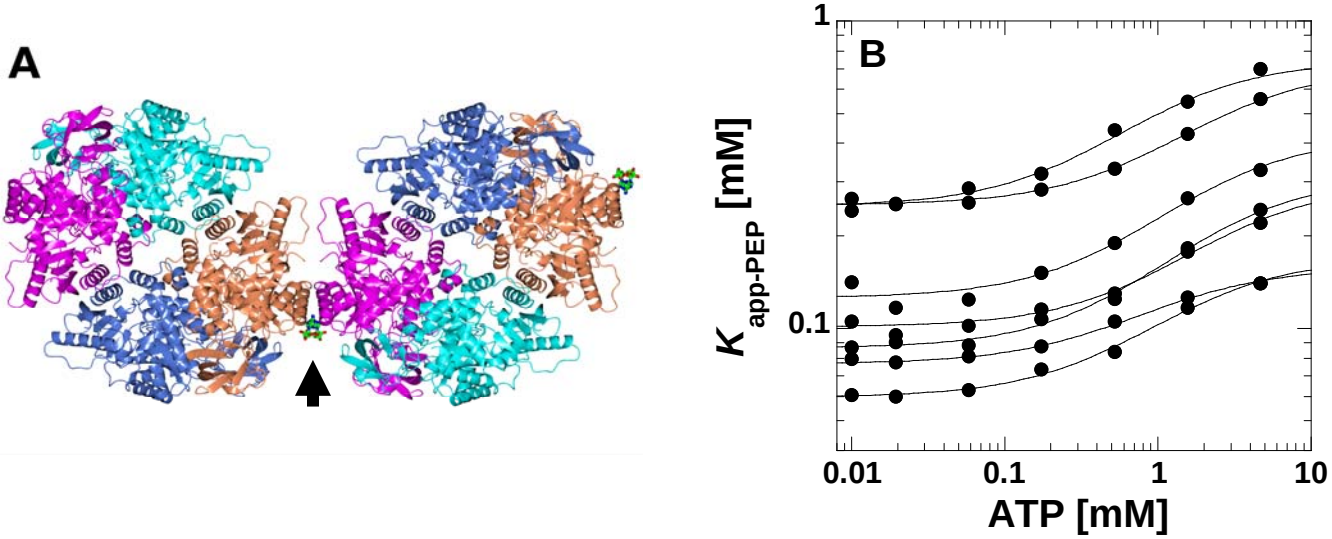

Other notable observations: Citrate in the active site

PYK is known to use ATP to phosphorylate a number of carboxylic acid containing ligands (*16*). Therefore to prevent turnover and the loss of ATP, no PEP, pyruvate or substrate analogue was added during crystallization. However, the citrate, used as a crystallization buffer, binds in the active site (Supportive Information). This finding may suggest that the inhibition of plant PYK isozymes by citrate (*17*) is a result of competitive binding between citrate and PEP.

A carboxylate from citrate occupies the same site as the carboxylate from PEP (i.e. coordination to the protein bound divalent cation). Citrate binding in the active site also explains the complete absence of neucleotide from the active site, since one of citrate's carboxylate groups bridges the binding sites for the α– and γ-phosphates of ATP. This observation also suggests that citrate should bind competitively with both PEP and ADP. In Supportive Information, competitive binding of citrate with both PEP and ADP has been confirmed using $K_{app\text{-}PEP}$ values determined from initial velocity data. However, the low affinity of L-PYK for citrate (K_{ix}>12mM) likely precludes this inhibition from having physiological significance in the liver.

Figure S5. A) The location and orientation of the molecule of citrate bound in the active site of L-PYK. The residues and metal ions that frame the binding site are illustrated and labeled accordingly. Fo-Fc density rendered at 4σ prior to inclusion of citrate into the model is shown as a blue mesh. B) Competitive inhibition of citrate on both PEP and ADP affinities in the active site. Lines represent the best fits to a competitive binding equation (*18*).

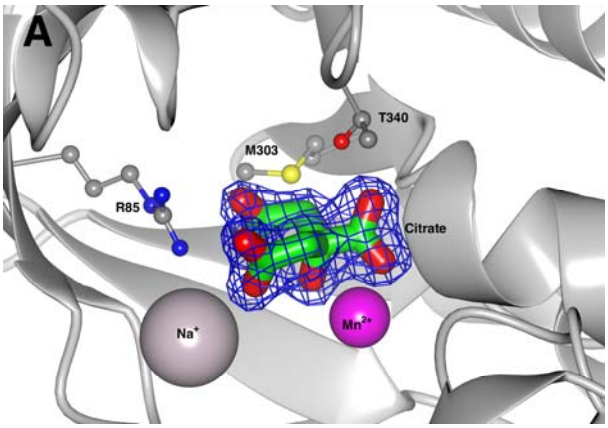

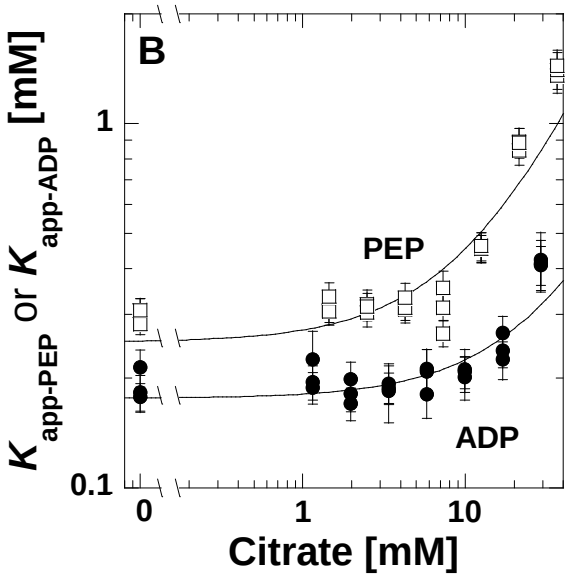

Other notable observations: Fru-1,6-BP binding orientation

The binding orientation of Fru-1,6-BP has previously been debated (*19-21*). This debate revolves around the nearly symmetrical structure of Fru-1,6-BP, with the exception of the location of the hydroxyl substituent at the anomeric carbon. Density for Fru-1,6-BP indicates a binding orientation with the 1'-phosphate of Fru-1,6-BP orientated towards Arg501 (Supportive Information). Despite the debate since the original co-crystallization study using yeast PYK (*20*), all subsequent work has confusingly claimed agreement with the binding orientation originally described in the yeast isozyme (*19, 21*). The source of this confusion appears to be a text vs. figure disagreement in the description of the binding site of yeast PYK (*20*). A comparison of the electron densities for all PYK isozymes with bound Fru-1,6-BP and that are deposited in the protein data bank indicate that there is no disagreement at the electron density level. Therefore, Fru-1,6-BP binds to yeast-PYK, human M_2-PYK, human R-PYK and L-PYK with the 1'-phosphate directed towards the equivalent of Arg501.

Figure S6. The binding orientation of Fru-1,6-BP. The bound Fru-1,6-BP is rendered as sticks and colored by atom type. 2Fo-Fc density rendered at 1.5σ is shown as a blue mesh. R501 is rendered as a ball-and-stick model colored by atom type.

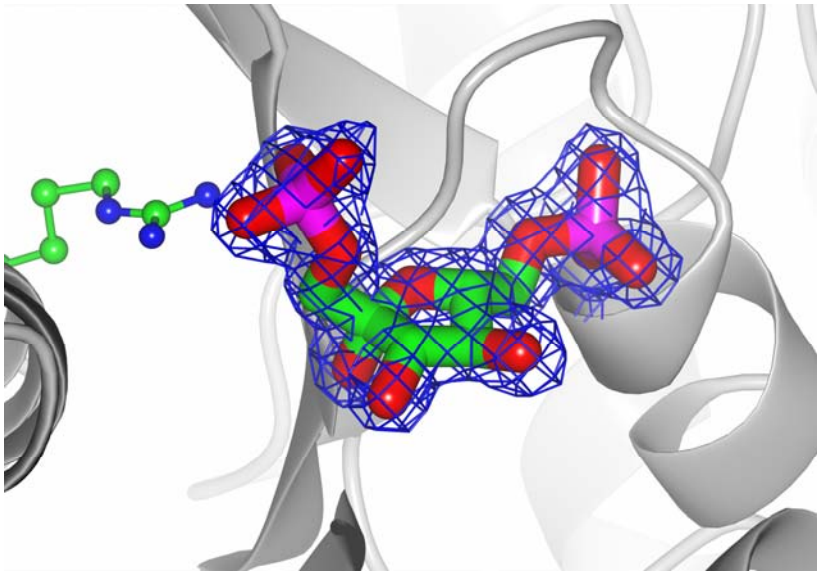

Table SI
Data for alanine-scanning mutagenesis used to generate Figure 5

Residue number	Residue type	Protein design[a]	$K_{a\text{-}PEP}$ (measured)	ΔG_{PEP} (measured)	$\Delta G_{PEP\text{-}WT}$ - $\Delta G_{PEP\text{-}mutant}$ (measured)
		Wild type	0.24±0.01	0.86±0.03	
Window of one alanine					
Residue number	Residue type	Protein design[a]	$K_{ia\text{-}PEP}$ (measured)	ΔG_{PEP} (measured)	$\Delta G_{PEP\text{-}WT}$ - $\Delta G_{PEP\text{-}mutant}$ (measured)
1	M				
2	E	E2A	0.20±0.01	0.96±0.04	-0.10±0.05
3	G	Wild type	0.24±0.01	0.86±0.03	0
4	P	P4A	0.25±0.02	0.83±0.04	0.29±0.05
5	A	Wild type	0.24±0.01	0.86±0.03	0
6	G	Wild type	0.24±0.01	0.86±0.03	0
7	Y	Y7A	0.20±0.02	0.97±0.05	-0.11±0.05
8	L	L8A	0.31±0.02	0.71±0.05	0.15±0.05
9	R	R9A	0.30±0.03	0.72±0.06	0.14±0.07
10	R	R10A	0.29±0.02	0.75±0.04	0.11±0.04
11	A	Wild type	0.24±0.01	0.86±0.03	0
12	S	S12A	0.097±0.010	1.40±0.06	-0.54±0.06
13	V	V13A	0.27±0.02	0.78±0.05	0.08±0.08
14	A	Wild type	0.24±0.01	0.86±0.03	0
15	Q	Q15A	0.18±0.02	1.04±0.06	-0.18±0.07
16	L	L16A	0.35±0.02	0.63±0.04	0.23±0.05
17	T	T17A	0.16±0.01	1.11±0.05	-0.25±0.06
18	Q	Q18A	0.11±0.02	1.30±0.08	-0.44±0.09
19	E	E19A	0.24±0.04	0.87±0.09	-0.01±0.09
20	L	L20A	0.50±0.03	0.42±0.03	0.44±0.04
21	G	Wild type	0.24±0.01	0.86±0.03	0
22	T	T22A	0.17±0.01	1.08±0.05	-0.22±0.06
23	A	Wild type	0.24±0.01	0.86±0.03	0
24	F	F24A	0.47±0.02	0.46±0.02	0.40±0.03

Window of two consecutive alanines[b]

Residue number	Residue type	Protein design[a]	$K_{a\text{-}PEP}$ (measured)	ΔG_{PEP} (measured)	$\Delta G_{PEP\text{-}WT}$ - $\Delta G_{PEP\text{-}mutant}$ (measured)	$\Delta\Delta G_{PEP}$ The sum of free energy differences caused by individual mutations from above
1	M					
2	E	E2A	0.20±0.01	0.96±0.04	-0.10±0.05	-0.10±0.06
3	G	P4A	0.25±0.02	0.83±0.04	0.29±0.05	0.03±0.06
4	P	P4A	0.25±0.02	0.83±0.04	0.29±0.05	0.03±0.06
5	A	Wild type	0.24±0.01	0.86±0.03	0	0
6	G	Y7A	0.20±0.02	0.97±0.05	-0.11±0.05	-0.11±0.07
7	Y	Y7A/L8A	0.27±0.01	0.79±0.01	0.07±0.03	0.04±0.08
8	L	L8A/R9A	0.33±0.01	0.66±0.01	0.20±0.03	0.29±0.09
9	R	R9A/R10A	0.47±0.01	0.45±0.02	0.41±0.03	0.25±0.08
10	R	R10A	0.29±0.02	0.75±0.04	0.11±0.04	0.11±0.06
11	A	S12A	0.097±0.010	1.40±0.06	-0.54±0.06	-0.54±0.07
12	S	S12A/V13A	0.22±0.01	0.90±0.01	-0.04±0.03	-0.47±0.08
13	V	V13A	0.27±0.02	0.78±0.05	0.08±0.05	0.08±0.07
14	A	Q15A	0.28±0.02	1.04±0.07	-0.18±0.07	-0.18±0.08
15	Q	Q15A/L16A	0.35±0.01	0.63±0.01	0.23±0.03	0.05±0.08

16	L	L16A/T17A	0.17±0.02	1.06±0.06	-0.20±0.07	-0.02±0.07
17	T	T17A/Q18A	0.16±0.01	1.12±0.01	-0.26±0.03	-0.7±0.1
18	Q	Q18A/E19A	0.17±0.01	1.07±0.02	-0.21±0.04	-0.5±0.1
19	E	E19A/L20A	0.29±0.01	0.74±0.01	0.12±0.03	0.4±0.1
20	L	L20A	0.50±0.03	0.42±0.03	0.44±0.04	0.44±0.05
21	G	T22A	0.17±0.01	1.08±0.05	-0.22±0.06	-0.22±0.07
22	T	T22A	0.17±0.01	1.08±0.05	-0.22±0.06	-0.22±0.07
23	A	F24A	0.47±0.02	0.46±0.02	0.40±0.03	-0.40±0.05
24	F	F24A/F25A	0.37±0.01	0.60±0.01	0.26±0.03	-0.40±0.05

Window of three consecutive alanines[c]

Residue number	Residue type	Protein design[a]	$K_{a\text{-}PEP}$ (measured)	ΔG_{PEP} (measured)	$\Delta G_{PEP\text{-}WT}$ - $\Delta G_{PEP\text{-}mutant}$ (measured)
1	M				
2	E	E2A/P4A	0.17±0.01	1.08±0.01	-0.21±0.03
3	G	P4A	0.25±0.02	0.83±0.04	0.29±0.05
4	P	P4A	0.25±0.02	0.83±0.04	0.29±0.05
5	A	Y7A	0.20±0.02	0.97±0.05	-0.11±0.05
6	G	Y7A/L8A	0.27±0.01	0.79±0.01	0.07±0.03
7	Y	Y7A/L8A/R9A	0.49±0.01	0.43±0.01	0.42±0.03
8	L	L8A/R9A/R10A	0.56±0.01	0.35±0.01	0.51±0.03
9	R	R9A/R10A	0.47±0.01	0.45±0.02	0.41±0.03
10	R	R10A/S12A	0.12±0.01	1.26±0.02	-0.40±0.03
11	A	S12A/V13A	0.22±0.01	0.90±0.01	-0.04±0.03
12	S	S12A/V13A	0.22±0.01	0.90±0.01	-0.04±0.03
13	V	V13A/Q15A	0.31±0.01	0.70±0.01	0.15±0.03
14	A	Q15A/L16A	0.35±0.01	0.63±0.01	0.23±0.03
15	Q	Q15A/L16A/T17A	0.23±0.01	0.88±0.01	-0.02±0.03
16	L	L16A/T17A/Q18A	0.29±0.01	0.75±0.01	0.11±0.03
17	T	T17A/Q18A/E19A	0.15±0.01	1.14±0.02	-0.28±0.03
18	Q	Q18A/E19A/L20A	0.47±0.01	0.45±0.01	0.41±0.03
19	E	E19A/L20A	0.29±0.01	0.74±0.01	0.12±0.03
20	L	L20A/T22A	0.48±0.01	0.44±0.01	0.42±0.03
21	G	T22A	0.17±0.01	1.08±0.05	-0.22±0.06
22	T	T22A/F24A	0.32±0.01	0.68±0.01	0.18±0.03
23	A	F24A/F15A	0.37±0.01	0.60±0.01	0.26±0.03
24	F				

[a]Due to the presence of alanine and glycine residues in the wild type sequence, the representative data may not involve a unique mutant design. Example 1, a single alanine at position 9 is equivalent to wild type and the data for the wild type protein is included in the protein design column, as opposed to a mutation. Example 2, the window for three consecutive alainies from positions 9-11 involves introducing alanine substitutions at positions 9 and 10, but no mutation at position 11; data for the R9A/R10A protein is used the protein design for the 9-11 entry for the three alanine-window from 9-11. When a unique mutation is not needed (i.e. data is used from an earlier entry into the table), data are highlighted in grey.

[b]Data for the window of two consecutive alanines are listed according to the first position of the window.

[c]Data for the window of three consecutive alanines are listed according to the first position of the window.

References

1. Blair, J. B. (1980) Regulatory Properties of Hepatic Pyruvate Kinase, In *The Regulation of Carbohydrate Formation and Utilization in Mammals* (Veneziale, C. M., Ed.), pp 121-151, University Park Press, Baltimore.
2. Irving, M. G., and Williams, J. F. (1973) Kinetic studies on the regulation of rabbit liver pyruvate kinase, *Biochem J 131*, 287-301.
3. Fenton, A. W., and Hutchinson, M. (2009) The pH dependence of the allosteric response of human liver pyruvate kinase to fructose-1,6-bisphosphate, ATP, and alanine, *Arch Biochem Biophys 484*, 16-23.
4. Fenton, A. W., and Alontaga, A. Y. (2009) The impact of ions on allosteric functions in human liver pyruvate kinase, *Methods Enzymol 466*, 83-107.
5. Stammers, D. K., and Muirhead, H. (1975) Three-dimensional structure of cat muscle pyruvate kinase at 6 Angstrom resolution, *J Mol Biol 95*, 213-225.
6. Srivastava, L. K., and Baquer, N. Z. (1985) Purification and properties of rat brain pyruvate kinase, *Arch Biochem Biophys 236*, 703-713.
7. Tsao, M. U. (1979) Kinetic properties of pyruvate kinase of rabbit brain, *Mol Cell Biochem 24*, 75-81.
8. Nicholas, P. C., and Bachelard, H. S. (1974) Kinetic properties of cerebral pyruvate kinase, *Biochem J 141*, 165-171.
9. Baranowska, B., and Baranowski, T. (1982) Kinetic properties of human muscle pyruvate kinase, *Mol Cell Biochem 45*, 117-125.
10. Terlecki, G. (1989) Purification and properties of pyruvate kinase type M1 from bovine brain, *Int J Biochem 21*, 1053-1060.
11. Baranowska, B., Terlecki, G., and Baranowski, T. (1984) The influence of inorganic phosphate and ATP on the kinetics of bovine heart muscle pyruvate kinase, *Mol Cell Biochem 64*, 45-50.
12. Larsen, T. M., Benning, M. M., Rayment, I., and Reed, G. H. (1998) Structure of the bis(Mg2+)-ATP-oxalate complex of the rabbit muscle pyruvate kinase at 2.1 A resolution: ATP binding over a barrel, *Biochemistry 37*, 6247-6255.
13. Morgan, H. P., McNae, I. W., Nowicki, M. W., Hannaert, V., Michels, P. A., Fothergill-Gilmore, L. A., and Walkinshaw, M. D. (2010) Allosteric mechanism of pyruvate kinase from Leishmania mexicana uses a rock and lock model, *J Biol Chem 285*, 12892-12898.
14. Fenton, A. W. (2008) Allostery: an illustrated definition for the 'second secret of life', *Trends Biochem Sci 33*, 420-425.
15. Reinhart, G. D. (2004) Quantitative analysis and interpretation of allosteric behavior, *Methods Enzymol 380*, 187-203.
16. Ash, D. E., Goodhart, P. J., and Reed, G. H. (1984) ATP-dependent phosphorylation of alpha-substituted carboxylic acids catalyzed by pyruvate kinase, *Arch Biochem Biophys 228*, 31-40.
17. Hu, Z., and Plaxton, W. C. (1996) Purification and characterization of cytosolic pyruvate kinase from leaves of the castor oil plant, *Arch Biochem Biophys 333*, 298-307.

18. Johnson, J. L., and Reinhart, G. D. (1997) Failure of a two-state model to describe the influence of phospho(enol)pyruvate on phosphofructokinase from Escherichia coli, *Biochemistry 36*, 12814-12822.
19. Dombrauckas, J. D., Santarsiero, B. D., and Mesecar, A. D. (2005) Structural basis for tumor pyruvate kinase M2 allosteric regulation and catalysis, *Biochemistry 44*, 9417-9429.
20. Jurica, M. S., Mesecar, A., Heath, P. J., Shi, W., Nowak, T., and Stoddard, B. L. (1998) The allosteric regulation of pyruvate kinase by fructose-1,6-bisphosphate, *Structure 6*, 195-210.
21. Valentini, G., Chiarelli, L. R., Fortin, R., Dolzan, M., Galizzi, A., Abraham, D. J., Wang, C., Bianchi, P., Zanella, A., and Mattevi, A. (2002) Structure and function of human erythrocyte pyruvate kinase. Molecular basis of nonspherocytic hemolytic anemia, *J Biol Chem 277*, 23807-23814.